AD-A149 849 TWO-DIMENSIONAL MEASUREMENTS OF OH CONCENTRATION AND TEMPERATURE IN REACTIVE FLOWS(U) SRI INTERNATIONAL MENLO PARK CA M J DYER ET AL. 05 DEC 84 1/1

UNCLASSIFIED AFWAL-TR-84-2045 F33615-81-K-2033 F/G 21/2 NL

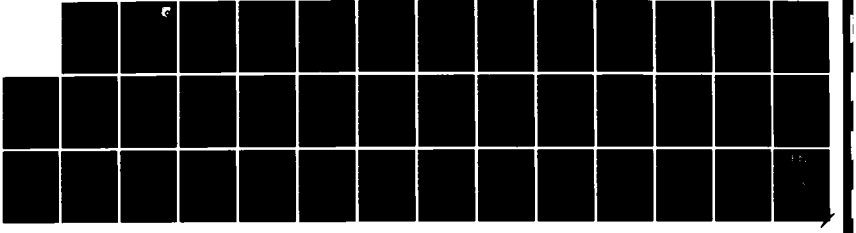

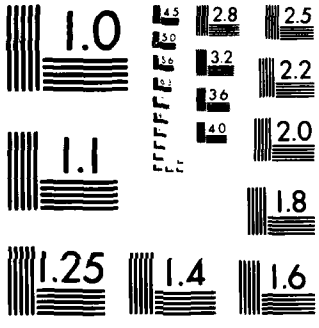

AFWAL-TR-84-2045

TWO-DIMENSIONAL MEASUREMENTS OF OH CONCENTRATION AND TEMPERATURE IN REACTIVE FLOWS

Mark J. Dyer, David R. Crosley

SRI INTERNATIONAL
MOLECULAR PHYSICS DEPARTMENT
333 RAVENSWOOOD AVENUE
MENLO PARK, CALIFORNIA 94025

DECEMBER 1984

FINAL REPORT FOR PERIOD JULY 1981 - MARCH 1984

AERO PROPULSION LABORATORY
AIR FORCE WRIGHT AERONAUTICAL LABORATORIES
AIR FORCE SYSTEMS COMMAND
WRIGHT-PATTERSON AIR FORCE BASE, OHIO 45433

NOTICE

When Government drawings, specifications, or other data are used for any purpose other than in connection with a definitely related Government procurement operation, the United States Government thereby incurs no responsibility nor any obligation whatsoever; and the fact that the government may have formulated, furnished, or in any way supplied the said drawings, specifications, or other data, is not to be regarded by implication or otherwise as in any manner licensing the holder or any other person or corporation, or conveying any rights or permission to manufacture use, or sell any patented invention that may in any way be related thereto.

This report has been reviewed by the Office of Public Affairs (ASD/PA) and is releasable to the National Technical Information Service (NTIS). At NTIS, it will be available to the general public, including foreign nations.

This technical report has been reviewed and is approved for publication.

Alan Garscadden

ALAN GARSCADDEN
Research Physicist

Wayne S. Bishop

WAYNE S. BISHOP, Acting Branch Chief
Batteries and Fuel Cells

FOR THE COMMANDER

PAUL R. BERTHEAUD
Dep Dir. Aerospace Power Division
Aero Propulsion Laboratory

"If your address has changed, if you wish to be removed from our mailing list, or if the addressee is no longer employed by your organization please notify AFWAL/POOC-3 *W-PAFB, OH 45433 to help us maintain a current mailing list".*

Copies of this report should not be returned unless return is required by security considerations, contractual obligations, or notice on a specific document.

UNCLASSIFIED

SECURITY CLASSIFICATION OF THIS PAGE

REPORT DOCUMENTATION PAGE

1a. REPORT SECURITY CLASSIFICATION UNCLASSIFIED	1b. RESTRICTIVE MARKINGS
2a. SECURITY CLASSIFICATION AUTHORITY	3. DISTRIBUTION/AVAILABILITY OF REPORT Approved for public release; distribution unlimited
2b. DECLASSIFICATION/DOWNGRADING SCHEDULE	
4. PERFORMING ORGANIZATION REPORT NUMBER(S)	5. MONITORING ORGANIZATION REPORT NUMBER(S) AFWAL-TR-84 -2045
6a. NAME OF PERFORMING ORGANIZATION SRI International 6b. OFFICE SYMBOL (If applicable)	7a. NAME OF MONITORING ORGANIZATION Aero Propulsion Laboratory (AFWAL/POOC)
6c. ADDRESS (City, State and ZIP Code) 333 Ravenswood Avenue Menlo Park, CA 94025	7b. ADDRESS (City, State and ZIP Code) Aero Propulsion Laboratory (AFWAL/POOC) Air Force Wright Aeronautical Laboratories (AFSC) Wright-Patterson Air Force Base, OH
8a. NAME OF FUNDING/SPONSORING ORGANIZATION 8b. OFFICE SYMBOL (If applicable)	9. PROCUREMENT INSTRUMENT IDENTIFICATION NUMBER F33615-81-K-2033
8c. ADDRESS (City, State and ZIP Code)	10. SOURCE OF FUNDING NOS. PROGRAM ELEMENT NO. 61102F; PROJECT NO. 2301; TASK NO. S1; WORK UNIT NO. 22
11. TITLE (Include Security Classification) Two-Dimensional Measurements of OH Concentration and Temperatures in Reactive Flows	
12. PERSONAL AUTHOR(S) Mark J. Dyer and David R. Crosley	
13a. TYPE OF REPORT Final Report 13b. TIME COVERED FROM 81/7 TO 84/3	14. DATE OF REPORT (Yr., Mo., Day) 1984/12/5 15. PAGE COUNT 71
16. SUPPLEMENTARY NOTATION	

17. COSATI CODES		
FIELD	GROUP	SUB. GR.
21	05	
20	04	

18. SUBJECT TERMS (Continue on reverse if necessary and identify by block number)
Laser-induced fluorescence, transfer ratios, quenching rates, rotational distributions.

19. ABSTRACT (Continue on reverse if necessary and identify by block number)

This report describes two related efforts that have as a common objective the development of new aspects of laser-induced fluorescence for measurements in time-varying reactive flows such as turbulent flames. The first effort was the demonstration, development and study of two-dimensional fluorescence imaging in flames. This provides a spatially correlated map of the concentration of OH radicals from a single laser shot. The second effort was the development of vibrational transfer thermometry, in which upward collisional energy transfer in the $A^2\Sigma^+$ state of laser excited OH in flames is used to measure temperature simultaneously with OH concentration. Although a good correlation (better than 5 per cent rms deviation) between measured intensities and temperature was obtained in the range 1400-2700K, it has not been possible thus far to place the method on a sound fundamental, theoretical footing.

20. DISTRIBUTION/AVAILABILITY OF ABSTRACT UNCLASSIFIED/UNLIMITED ☒ SAME AS RPT. ☐ DTIC USERS ☐	21. ABSTRACT SECURITY CLASSIFICATION Unclassified
22a. NAME OF RESPONSIBLE INDIVIDUAL CAPTAIN G.R. SCHNEIDER	22b. TELEPHONE NUMBER (Include Area Code) (513) 255-2923 22c. OFFICE SYMBOL AFWAL/POOC-3

DD FORM 1473, 83 APR EDITION OF 1 JAN 73 IS OBSOLETE.

UNCLASSIFIED

SECURITY CLASSIFICATION OF THIS PAGE

CONTENTS

FIGURES

TABLES

I INTRODUCTION

Laser-induced fluorescence (LIF) provides a sensitive means of detecting trace species, often free radicals, that are the reactive intermediates in combustion chemistry.[1] Qualitative identification can provide insights into the mechanism of that chemistry, while quantitative measurement yields data for comparison with computer models containing detailed kinetics. One of the attributes of LIF is its ability to provide spatially and temporally resolved information. Point-resolved measurements are made by focusing the fluorescence at right angles to the laser beam onto a slit oriented perpendicular to the beam propagation direction, whereas temporal resolution is inherent in the use of pulsed lasers. This has been the customary mode of acquisition of LIF data on stable flames where the burner is translated through the optical measurement point, so as to yield a profile of the pertinent species.

In a time-varying flow such as turbulent combustion, however, the system changes character at a given point between successive laser shots (which are typically separated by 100 msec for lasers used in such studies.) Thus a series of point measurements can be treated only statistically, in the form of probability distribution functions, for comparison with theoretical treatments. It would instead be highly desirable to obtain correlated information during a single laser pulse. Such information could take two forms: The spatial, multipoint distribution of some observable, or the measurement of two or more observables simultaneously. The two could, in principle, then be combined to determine the instantaneous spatial distribution of a pair of observables.

The demonstration, development, and study of methods to meet these needs has been the objective of this project. The instanteous spatial distribution of OH molecules in a flame can now be determined using the technique of two-dimensional fluorescence imaging, first performed by us in this work[2,3] and now in use in several laboratories around the world. The simultaneous measurement of OH concentration and the temperature has been addressed using the method of vibrational energy transfer,[4] although we have not been success-

ful in determining a foundation for implementing the method quantitatively for a range of flame conditions. The OH radical has been the subject of these studies. Ubiquitous in flames and important in many of the major and minor chemical pathways, the OH radical is often present in relatively large amounts (> 100 ppm) and its absorption lies in an experimentally convenient laser wavelength region. It is the key intermediate detectable by laser methods and the one most likely to be of interest in measurements on turbulent flames.

II TWO-DIMENSIONAL FLUORESCENCE IMAGING

Our efforts on the project were devoted to the demonstration and development of two-dimensional fluorescence imaging. This proceeded quickly and successfully, yielding the first signals in January 1982. Subsequent study and refinement of the method showed excellent sensitivity on single laser shots. Following our announcement of the demonstration, the method was successfully attempted elsewhere and is now in use in at least a half-dozen laboratories. The method and the results of our study of it were fully described in two papers[2,3].

III VIBRATIONAL ENERGY TRANSFER THERMOMETRY (VETT)

The objective of this phase of the work was the development of a method to provide, on a single laser shot with one laser, a simultaneous measurement of the OH concentration and the temperature. The concept of the method[4] is as follows.

Figure 1 depicts the energy levels and the radiative transitions involved in the experiment. A laser is tuned to the wavelength of a given absorption line of the (0,0) band of the $A^2\Sigma^+$-$X^2\Pi_1$ electronic transition, populating a particular rotational level in $v' = 0$. (The rotational levels are not shown explicitly in Figure 1.) While in the $A^2\Sigma^+$ state and before radiating, a few of the molecules excited by the laser undergo collisions, raising them into the $v' = 1$ vibrational level. Measurements of the intensities of the (0,0) and (1,0) bands, as indicated in the figure, furnish the ratio of the popula-

tions in the two vibrational levels, from which the temperature can be derived.

The population ratios reported in Ref. 4 were analyzed within the framework of a steady-state approximation. We consider only the total population in each vibrational level; that is, any influence of rotation on the vibrational transfer collisional processes is ignored. A steady-state balance applied to N_1 yields

$$[V \exp(-\Delta E/kT)]N_o = (V + A + Q)N_1 \quad . \tag{1}$$

Here (see Fig. 3), the downward vibrational transfer rate is V, and the upward transfer is given by detailed balancing as $V \exp(-\Delta E/kT)$. Q is the quench rate, and A is the Einstein emission coefficient for $v' = 1$. Since $A/(V + Q) < 0.01$, A was ignored. Rearranging,

$$\frac{N_1}{N_o} = \frac{\exp(-\Delta E/kT)}{1 + Q/V} \tag{2}$$

or

$$T = -\frac{\Delta E}{k} \quad \ln \quad (1 + Q/V)\frac{N_1}{N_o}^{-1} \quad . \tag{3}$$

Thus from the measured ratio and a value of Q/V, one may determine the temperature.

The method was originally demonstrated[4] using point measurements in the burnt gases of CH_4/air flames. Temperatures T_V measured by VETT were found to agree well with measurements of the ground state rotational temperatures T_R obtained via excitation scans (after subsequent corrections[5] to each were applied, necessary because of the neglect of rotational transfer effects[6] on T_R and an incorrect estimate[5] of Q/V in Ref. 4). Good agreement (within 10%) was achieved between T_V measured following excitation of three different rotational levels in $v' = 0$ [$F_1(4)$, $F_2(10)$, $F_2(14)$]. Using split images and separately filtered vidicon halves, we could in principle use this method in an imaging experiment to yield an instantaneous map of the OH concentration and temperature throughout those regions of the flame where OH was present.

Following the demonstration of VETT in Ref. 4, several questions remained concerning its applicability in a quantitative way, for a range of temperatures and flame gas collisional environments. These are

(1) Given the knowledge of rotational-state-specific vibrational energy transfer in $A^2\Sigma^+OH$, both in room temperature flows[7] and in flames,[5] what are the effects of pumping different N' levels in v' = 0 and measuring only part of the rotational distribution in v' = 1?

(2) How does the parameter Q/V (needed for the analysis) vary with the collisional environment, both gas mixture and temperature?

(3) Over what range of temperature can one reliably measure T_V and what is its precision, compared to nonintrusive laser measurements of T_R as well as thermocouple measurements that furnish T_{tc} but are intrusive and require radiative corrections?

These questions have been addressed by a series of single-point, multi-pulse averaged measurements in the burnt gases of stable flames of $CH_4/O_2/air$. These flames have furnished a temperature range of about 1400 to 2700K with high enough OH densities to produce usable signals.

A. Signal Analysis Equations: Determination of Q/V

Eq. (3) was derived under two assumptions: first, a steady state treatment of the populations and, second, that the quenching rate Q_o from v' = 0 is the same as the quench rate Q_1 from v' = 1 (each denoted by Q). We here consider the time-dependent equations that describe the actual experiment.

Neglecting rotational level effects, the pertinent equations are: (i) Uptransfer, pumping v' = 0:

$$\frac{dN_o}{dt} = L(t) - Q_oN_o \tag{4}$$

$$\frac{dN_1}{dt} = Ve^{-\Delta E/kT} N_o - Q_1N_1 - VN_1 \tag{5}$$

$$R_u = \int_o^\infty N_1(t)dt / \int_o^\infty N_o(t)dt \tag{6}$$

(ii) Downtransfer, pumping v' = 1:

$$\frac{dN_1}{dt} = L(t) - VN_1 - Q_1N_1 \tag{7}$$

$$\frac{dN_o}{dt} = VN_1 - Q_oN_o \tag{8}$$

$$R_D = \int_o^\infty N_o(t)dt / \int_o^\infty N_1(t)dt \tag{9}$$

Here, L(t) is the time-dependence of the laser pulse; it is conveniently and realistically expressed as the difference of two exponentials: $L(t) = e^{-\ell_1 t} - e^{-\ell_2 t}$. In the experiment, we use a gated boxcar integrator whose output is proportional to the intensity of some band [(1,0), (1,1) or (0,0)] from which is obtained the population of the corresponding v' level. The detector time constants are much longer than the inverses of ℓ_1, ℓ_2, or the collisional rates involved. Thus the boxcar output yields $\int_o^\infty N_1(t)dt$ and the measured band ratios are those given by R_u and R_D.

An equation of general form

$$\frac{dx}{dt} = \sum_i k_i \exp(-a_i t) - cx \tag{10}$$

is solved by

$$x = \sum_i \frac{k_i}{c - a_i} \left[\exp(-a_i t) - \exp(-ct) \right] \tag{11}$$

and has

$$\int_o^\infty x dt = \frac{1}{c} \sum_i \frac{k_i}{a_i} \tag{12}$$

Therefore,

$$R_D = \frac{Q_o}{V} \tag{13}$$

$$R_u = \frac{V \exp(-\Delta E/kT)}{V + Q_1} \tag{14}$$

Note that Q_0, the quenching rate for v' = 0, is determined by the downward transfer experiment pumping v' = 1, whereas Q_1, the quenching rate for v' = 1, is needed for analysis of the v' = 0 pump uptransfer runs used to determined the temperature.

B. Experimental Arrangement

The experiments described in the succeeding sections were all performed using point-resolved measurements in the burnt gases of premixed $CH_4/O_2/N_2$ flames at atmospheric pressure. The burner was 1 cm in diameter; its surface consisted of a plate drilled with 1-mm-d holes to ensure even flows in the burnt gas region. The horizontal laser beam, 1 mm in diameter, passed across the burner and the fluorescence was focused at right angles onto the vertical slit of a 3/4-m spectrometer. Slit widths ranging from 0.1 to 3 mm were used, depending on the experiment conducted. The fluorescence was detected with an EMI 9558QA photomultiplier. In a few excitation scan runs, total undispersed fluorescence was collected with a filtered 1P28A photomultiplier viewing the center of the flame. The photomultiplier output in each case was fed to a boxcar integrator. The boxcar output in turn was recorded on a strip chart recorder for some runs; for other runs the output was stored in the Molecular Physics Laboratory computer through a remote hookup.[8] The flames were generally slightly rich (Φ=1.1 to 1.2) mixtures of CH_4, O_2, and air. The flows were measured with rotameters that had been calibrated with a wet test meter. According to equilibrium calculations,[9] the OH concentration varied from ~ 30 to ~ 1500 ppm over the series of mixtures used; occasionally, absorption measurements were made that confirmed these values. Tests were made to ensure operation in regions of the flame where absorption by OH of the laser light or the fluorescence did not pose problems.

C. Rotational Distributions for Uptransferred OH

In this phase of the study, we measured the rotational distributions of OH molecules that had been collisionally transferred upwards from v' = 0 to v' = 1. Individual rotational levels within v' = 0 were pumped by the laser, and rotationally resolved fluorescence scans were made of the (1,0) band in fluorescence to determine relative populations among the rotational levels in v' = 1. This information is needed to ascertain the spread of the spectrum,

to set wavelength observation limits for the less well-resolved thermometry runs, to choose the pertinent N' in v' = 1 that should be pumped to measure a pertinent Q/V in the downward transfer measurements, and to address questions concerning possible N' variation of both Q and V that may enter into the data interpretation.

Using a variety of slit widths furnishing resolution between 0.2 and 1 Å, we obtained fluorescence spectra in the burnt gas regions where excitation scans showed the rotational temperature $T_R \sim 2100K$. A sample spectrum is shown in Figure 2. From such spectra, 50 spectral "features", definable peaks or shoulders, were identified and their intensities measured. Each of these features is composed of from 1 to 8 known rotational lines of the (1,0) band, the exact mix depending on the spectrometer bandwidth used for the particular run. The intensities are then interpreted in terms of relative populations of the 31 rotational levels, $F_1(N')$ and $F_2(N')$ for N' = 0 to 15. An analysis program was written using listed line positions[10] and line strengths.[11] The spectrometer bandwidth $\Delta\lambda$ could be varied over appropriate limits, and a least squares fit to the populations was made. For example, in some of the earlier lower resolution runs, a variation of the assumed $\Delta\lambda$ between 0.80 and 0.95 Å reduced the χ^2 value by 30%. Most of the later runs were made with higher resolution, near 0.2 Å, where only 1 or 2 levels contributed significantly to each chosen feature.

The results from pumping a series of levels are shown in Figure 3 in the form of Boltzmann plots for ready comparison with T_R. There is some scatter at the lowest N', due to low intensities for the pertinent features and consequent ill-conditioning in the fit; this scatter does not, however, affect the essential conclusions and no real effort was made to improve the fitting procedure to accommodate the problem.

We may conclude that, within experimental error, the population distribution of the uptransferred molecules is near-Boltzmann in nature, described reasonably by a temperature very close to the gas temperature, and has no significant dependence on the originally pumped level in v' = 0. Note that the N' = 5 and 6 levels have but 500-700 cm^{-1} of rotational energy, whereas N' = 12 and 13 are at 2600 and 3000 cm^{-1} above N' = 0 of v' = 0; these latter energy levels may be compared with $\Delta G_{1/2}$ of the $A^2\Sigma^+$ state, which is 2990 cm^{-1}.

These results in turn suggest that downtransfer experiments pumping $N' = 6$ in $v' = 1$, which is the most highly populated rotational level in this temperature region, should well simulate the collisional behavior of the upward transferred OH, assuming that enough rotational redistribution takes place following the initial excitation of $N' = 6$.

D. Upward Transfer as a Function of Rotational Level in $v' = 0$

In the initial VETT experiments,[4] measurements of the degree of upward $0 \rightarrow 1$ transfer were made by pumping different rotational levels. The results for $N' = 4$, 10, and 13 showed the same degree of transfer within experimental error. This was surprising, for it might have been anticipated that the additional rotational energy would facilitate the endoergic transfer. (Downward transfer has been shown[5] to decrease with increasing N' in $v' = 1$). We have carried out a more definitive set of scans, in two different flames, and find results conflicting with those of Ref. 4. Here, the upward transfer ratio of N_1/N_o was measured and found to vary smoothly with N'. We do not understand the disagreement with the results of Ref. 4, although a slightly different flame environment was used in the current scans.

The first set of runs was made on downward transfer to check the correction for band overlap. The (1,1) band head is at 3122 Å. P branches of the (0,0) band for $N' > 8$ and Q branches for $N' > 15$ are to the red of this wavelength. Thus the measured intensity between 3064 and 3122 Å represents only a fraction f of the true (0,0) intensity, while that from 3122 Å onward to the red includes all of the (1,1) band plus 1-f of the (0,0) band. Since the fraction of molecules with quantum number J_o or greater at some temperature T is

$$\int_{J_o}^{\infty} (2J + 1)e^{-BJ(J + 1)/kT} dJ / \int_{o}^{\infty} (2J + 1)e^{-BJ(J + 1)/kT} dJ \qquad (15)$$

$$= e^{-BJ_o(J_o + 1)/kT} ,$$

f may be evaluated; for a 2200K thermal distribution it is 0.85. Using this correction for the (1,1) band, measurements were made of the $v' = 1$ population using both the (1,0) and the (1,1) band intensities. Needed are the spectro-

meter and photomultiplier responses at the respective wavelengths; these are taken from manufacturers' curves for our EMI tube and Bausch and Lomb grating. Also needed are the relative Einstein coefficients for the two bands.[12] The results for the two bands yield N_1 = 22.08 and 21.95, agreeing better than the estimated intensity uncertainties and indicating that the correction is properly accounted for.

Measurements of the upward transfer ratio N_1/N_o were then made in two separate flames: cool (1650K) and hot (2800K), where the temperatures were determined by excitation scans. Exemplary data are shown in Figure 4. In each case three different rotational levels were pumped. The results are given in Table 1. Note that the two $Q_1 9$ runs for the cool flame and the $Q_1 9$, $P_1 10$ pair for the hot flame constitute replicate runs because in each case the same upper level, $F_1(9)$, is excited. The agreement for these pairs is excellent.

In each case the hotter flame shows more upward transfer, as expected. However, the N_1/N_o ratio increases smoothly with increasing N' in v' = 0, in contrast to the results of Ref. 4. We did not attempt to address this discrepancy. Neither did we pursue the interesting fundamental questions posed by these results concerning the efficacy of rotational energy in promoting upward vibrational transfer at the expense of large changes in angular momentum. Rather, we decided to conduct the remainder of the experiments pumping N' = 6, J' = 61/2, in both v' = 0 for upward transfer and v' = 1 for downward transfer. This is the most highly populated level for thermal populations near 2000K and in the rotational distribution of upward transferred molecules, as described in the preceding section. The behavior of the N' = 6 level should therefore be reasonably considered as that of an average N' value, given a smooth variation in collision rate with N', and the effects of any rotational redistribution that does occur will be minimized.

E. Final Q/V and Thermometry Runs

In this section we describe our final set of runs measuring T, Q/V, and N_1/N_o in a series of flames.

(1) *Flames Used*. A series of three flames were probed so as to produce different but overlapping temperature ranges, although each had a slightly

Table 1

N_1/N_o RESULTS FOR UPWARD TRANSFER FOR DIFFERENT PUMP LINES

Line	Cool flame	Hot flame
$P_2 1'$	0.0327	0.0417
$Q_1 9$	0.0406	-
$Q_1 9$	0.0456	0.0498
$P_1 10$	-	0.0499
$Q_1 13$	0.0527	0.0612

varying collisional mix in the burnt gas region. The flows of methane, oxygen, and air used are given in Table 2; we shall denote the flames as H, M and L in the following, in spite of the temperature overlap. Operation at different points (heights above the burner) in the burnt gases yielded a wide range of usable temperatures, from 1400 to 2700K.

(2) Temperature Determination by Thermocouples and Excitation Scans[13]. We devoted considerable effort to ensuring that we could accurately determine the gas temperature at different points. First, a series of excitation scans was made to determine T_R. Early replicate runs showed disagreement outside fitting errors, but this was found to be due to optical depth problems. A typical Boltzmann plot from one of the later runs is shown in Figure 5. Except for the lowest P-branches, the data fit with standard deviations of 3-5%. The P-branch discrepancy may be due to polarization effects[14] but the cause was not investigated here, and the Q-branch sequence was used to determine T_R.

An extensive series of thermocouple measurements was made in each flame. Four thermocouples of varying bead size (nominal diameter 0.002", 0.005", 0.015", and 0.020") were used to provide related values of the radiative correction. Measurements were made at as many as 40 points in each flame for each thermocouple, at different positions through the burnt gas region as close to the flame zone as survival of the thermocouple would permit. A series of measurements is shown in Figure 6.

A radiative correction is necessary because of emissive heat loss from the thermocouple. The gas temperature T_g is related to the bead temperature by

$$T_g = T_b + \frac{\sigma \varepsilon D \left(T_b^4 - T_w^4\right)}{kNu} \qquad (16)$$

where σ is the Stefan-Boltzmann constant, D and ε the bead diameter and emissivity, k the gas thermal conductivity, Nu the Nusselt number, and T_w the temperature of the radiation sink (300K). Using the nominal bead diameters and $\varepsilon = 0.3$, we were unable to obtain consistency among T_g values calculated for each thermocouple at each point. Therefore, Eq. (16) was used in empirical form (noting $T_w^4 \ll T_b^4$):

Table 2

FLOW RATES (cm^3 sec^{-1}) AND OTHER PARAMETERS FOR FLAMES IN FINAL RUNS

	H	M	L
CH_4	12.7	9.78	6.52
O_2	13.5	11.9	0
Air	42	29.2	52.5
Φ	1.14	1.09	1.18
Temperature Range Used (K)	1900-2700	1600-2400	1300-2000

$$T_g = T_b + aD\ T_b^4 \quad . \qquad (2)$$

A single value of a was determined for all the measurements such that differences in T_g for the 0.002", 0.005", and (in the H and M flames) 0.015" thermocouples were minimized at each point. (The 0.020" set was not consistent.) The values of a so determined were $a_H = 1.33 \times 10^{-8}$, $a_m = 1.25 \times 10^{-8}$, $a_L = 1.51 \times 10^{-8}$ compared to a calculated value 0.66×10^{-8} from the constants of Eq. (16), all in units of $cm^{-1}\ K^{-4}$. The difference reflects primarily a larger effective bead diameter compared to the nominal value. A value $a = 1.32 \times 10^{-8}$ was used to reduce the remainder of the data. The resulting temperatures then agreed to within 1-3%. Results for the VETT measurement locations are given in Table 3. The highest-T values from the 0.015" thermocouple were not used when they clearly disagreed with those of the smaller bead devices. Values in parentheses are extrapolations from lower temperature along curves parallel to those of the larger thermocouples.

The results also agreed with excitation scan values of T_R at the same point. For example, at the 3.1 and 3.6 cm positions of flame H, we determined $T_{tc} = 2068 \pm 34K$, $T_R = 2032K$, and $T_{tc} = 2141 \pm 38K$, $T_R = 2157K$, respectively. The uncertainties in T_{tc} represent the spread in values obtained by applying Eq. (17) to the three thermocouples, all with $a = 1.32 \times 10^{-8}$.

In the following sections, Q/V and N_1/N_o measurements are described. These were made at a total of 20 spatial locations (6 in flame L, 9 in M, 5 in H). In each case N' = 6, J = 6.5 level was pumped in both v' = 0 and 1. The highest temperature point in L was clearly erroneous, because the finite-size laser beam partially covered a region of sharp temperature gradient in the reaction zone, and it is excluded from further discussion. The other 19 measurements are all included. At each spatial location, T_{tc} was determined using the procedure described in this section. This T_{tc} forms the value plotted on the abscissa of Figures 7-10.

(3) Q/V Results. The value of Q_o/V was determined from the degree of downward transfer (see Eq. 13). The method of Ref. 5 was used to analyze the population ratios from the intensities of the (1,0) and (0,0) bands, correcting the latter for the overlap with (1,1) as described above. The

Table 3

THERMOCOUPLE RESULTS (K) FOR $a = 1.32 \times 10^{-9}$

(Asterisk denotes not used; parentheses denote extrapolated value)

	ΔT			T		
Flame and Point	0.002"	0.005"	0.015"	0.002"	0.005"	0.015"
L1	64	144	-	1793	1824	-
L2	56	106	-	1728	1696	-
L3	44	88	-	1604	1574	-
L4	32	64	-	1476	1433	-
L5	24	50	-	1377	1341	-
M1	-	-	804	(2396)	(2403)	2765*
M2	-	293	644	(2290)	2298	2498*
M3	-	256	552	(2153)	2194	2337*
M4	115	220	468	2111	2087	2181*
M5	98	189	409	2015	1984	2065
M6	83	165	336	1925	1899	1913
M7	71	142	294	1842	1814	1819
M8	60	119	254	1756	1720	1724
M9	50	114	210	1668	1699	1612
H1	-	-	925	(2620)	(2700)	2956*
H2	-	-	711	(2450)	(2490)	2613*
H3	-	297	630	(2298)	2310	2475*
H4	121	232	491	2144	2123	2225*
H5	96	183	387	2005	1966	2021

results are listed in Table 4 and plotted in Figure 7 as a function of T_{tc} for the three flames.

A very large variation was seen because the v' = 0 rotational distribution may vary with gas temperature, and collisional quenching rates from v' = 0 are known to vary with N', according to measurements at room temperature.[15-17] Additionally the collisional environment varies slightly from flame to flame, although not enough to change Q_o as much as is seen here, according to measurements at room temperature[17] and elevated temperature[18] for a variety of collision partners. V also varies with collider gas according to room temperature data,[7,19] although vibrational transfer of $A^2\Sigma^+$ OH has never been measured for H_2O as a collision partner. The fact that all the points for a given flame, H, M and L, lie on a smooth line -- which is different for each flame -- suggests that differences in the collisional mixture is the cause of the Q/V variation. Nonetheless, the variation of Q/V is much greater than expected on these grounds.

(4) N_1/N_o results. Upward transfer runs were made at the same spatial locations of the Q/V measurements. Analysis was as described in Ref. 4 and Section IIIA; the results are listed in Table 4 and are plotted versus T_{tc} in Figure 8. Note that there is a smooth overall increase in N_1/N_o with increasing temperature, as anticipated.

F. Thermometry Results

(1) VETT Results. Eq. (3) was used to determine the temperature T_V at each measurement point, taking as input the experimental values of $R_D = Q/V$ and N_1/N_o. The results are listed in Table 5 and plotted versus T_{tc} in Figure 9. They do not make sense. Although N_1/N_o increases with temperature as expected, the increase in Q/V with T_{tc} (Figure 7) forces T_V to rise much too sharply and attain wholly unrealistic values.

(2) An Approach Using an Effective Value of Q/V). The lack of correspon dence of T_V with T_{tc} may be due to rotational dependences in the collision rates, or the fact that Q_o/V is measured by the downward transfer (Eq. 13), whereas Q_1/V is needed to obtain T_V (Eq. 14). The fact that relatively smooth variation is seen for each flame (Figures 7 and 8) encouraged us to try a

Table 4

RESULTS OF THERMOMETRY MEASUREMENTS

Flame	Measurement Point	T_{tc}	$N_1/N_o \times 10^2$	Q/V	T_V (Eq. 3)
L	1	1809	2.27	1.83	1519
	2	1712	2.26	1.70	1491
	3	1589	2.14	1.60	1443
	4	1455	1.63	1.25	1261
	5	1359	1.71	1.45	1314
M	1	2400	6.13	4.73	3987
	2	2294	5.31	4.34	3308
	3	2174	5.33	4.21	3254
	4	2099	4.67	3.69	2746
	5	2001	3.75	3.69	2399
	6	1912	4.10	3.44	2447
	7	1826	4.25	3.27	2443
	8	1738	3.13	2.98	2002
	9	1685	2.13	2.67	1636
H	1	2660	8.69	4.93	6290
	2	2470	7.37	4.25	4392
	3	2304	6.75	3.70	3632
	4	2133	5.82	3.40	3061
	5	1985	4.76	2.90	2476

different approach. The temperature at each point was equal to T_{tc}, and the measured ratio was then used to derive an effective Q/V by inverting the thermometry equation (3):

$$\frac{Q}{V}_{eff} = \frac{\exp\left(-\Delta E/kT_{tc}\right)}{N_1/N_o} - 1 \qquad (18)$$

The results from this step are given in Table 5.

Table 5 shows a definite ordering of the values of $(Q/V)_{eff}$ by flame. We thus considered that this parameter may be the same for all the points in a given flame, even though it may differ from flame to flame because of a different mixture of collision partners. Accordingly, average values $(\overline{Q/V})_{eff}$ were calculated. (Only 6 of the 9 points in the M flame were used; those not included in computing the average are marked with an asterisk in Table 5.) The results are $(\overline{Q/V})_{eff}$ = 2.57 ± 0 62 for L, 1.88 ± 0.12 for M, and 1.47 ± 0.07 for H. These are far from the values measured by downward transfer and are in fact in the opposite direction (compare Tables 4 and 5). We do not know the reasons for these differences.

Nonetheless we proceeded, applying the average $(\overline{Q/V})_{eff}$ for each flame to the measurements at all the points in that flame. With this a new, "calibrated" T_V (which we label T_c) was calculated using Eq. (3). The results are listed in Table 5 and plotted versus T_{tc} in Figure 10. Note that the scale is different from that in Figure 9.

These "calibrated" thermometry results are in very good agreement with T_{tc}, as seen by the straight line in Figure 10 which is the equation $T_c = T_{tc}$. For the 19 points, the standard deviation is 3.56% and rms deviation is 4.96%. In fact, 4 points with a deviation of 8% or more in $(T_c-T_{tc})/T_{tc}$ contribute about half of this uncertainty. In situ, spectroscopic flame temperature measurements with this level of accuracy can be considered excellent.

G. Summary and Discussion of Thermometry Results

In this study we first determined that we can make precise measurements of the temperature in the burnt gases of a methane/air flame, using rotational excitation scans and thermocouple measurements. This turned out to be a more

Table 5

"CALIBRATED" THERMOMETRY RESULTS

Flame	Measurement Point	T_{tc}	$(Q/V)_{eff}$	T_V (calibrated)
L	1	1809	3.39	1660
	2	1712	2.87	1657
	3	1589	2.39	1622
	4	1455	2.49	1466
	5	1359	1.72	1491
M	1	2400	1.87	2405
	2	2294	2.06	2181
	3	2174	1.76	2225
	4	2099	1.94	2079
	5	2001	2.32*	1874
	6	1912	1.75	1952
	7	1826	1.40*	1985
	8	1738	1.90	1733
	9	1685	2.95*	1494
H	1	2660	1.40	2710
	2	2470	1.51	2448
	3	2304	1.42	2328
	4	2133	1.43	2150
	5	1985	1.57	1948

*Points not included in computing average values of $(Q/V)_{eff}$ for the M flame.

painstaking task than first assumed. There existed ample opportunity for systematic errors in the T_R determinations, and the deviation of the low P-branches from the Boltzmann plot (Figure 5) indicates that we have not solved all of them. Only by fitting a series of thermocouple results, using varying bead sizes, were we able to attain a self-consistent set of radiative corrections. We are wary of any flame thermocouple measurements made with a single thermocouple using the nominal equation and constants of Eq. (16).

The VETT temperature T_V was then determined using both upward and downward transfer to determine, at the same locations, N_1/N_o and Q/V. Combining these to obtain T_V produced unrealistic results compared with the thermocouple measurements. The results make too little sense to warrant any statistical treatment.

However, using the set of measured N_1/N_o for each flame and knowledge of T_{tc}, an effective, averaged value of the Q/V parameter could be determined for each flame. Using these three values, the newly determined T_c agreed with T_{tc} over the 19 experimental points to within better than 5%. This means an average deviation of between 70 and 130K depending on the flame temperature, which varied from 1400 to 2700K. This is excellent agreement.

Why does the calibration method work? It appears that the effective value of Q/V is dependent on the collisional mix but not much on the temperature. It is very different from the values measured directly using the downward transfer. Part of the discrepancy may lie in the dependence of the rotational variation of the various collisional rates on different species. Also recall that Q_1/V is needed for the analysis of N_1/N_o in the thermometry equation, but Q_o/V is the quantity actually measured in the downward transfer. From low pressure measurements,[7,19] it is known that V depends on N' in $v' = 1$ and this shows up in flames as well.[5] Recent measurements in this laboratory[16,17] show that Q_o is N'-dependent. The dependence is true for a wide range of collision partners, but the degree of variation (always a decrease in Q_o with increasing N') is different from gas to gas. No definitive knowledge exists concerning variation of Q_1. Even though the upward-transferred rotational distribution is near thermal (Section III B), perhaps the N' dependence of these quantities over differing collisional mixes is simply too great for the directly measured Q/V to be applicable.

With calibration of the effective value of Q/V in a burnt gas collisional mixture, very good temperature determinations have been made. One can expect to measure temperatures with a typical precision of 100K in an exhaust gas system at 2000K, and, performed this way, VETT has definite promise as a flame thermometer. The lack of a fundamental understanding of the differences between the values of $(A/V)_{eff}$ and the measured Q/V, however, suggests extreme caution in setting limits of applicability of VETT to various flame gas environments.

Because of the lack of correspondence of the measured Q/V and the $(Q/V)_{eff}$ values determined by upward-transfer runs, we did not pursue the proposed three-channel thermometry, where $v' = 1$ is pumped and each of $v' = 0$, 1 and 2 is observed. This was in spite of the ability to discern further upward transfer $v' = 0 \rightarrow 1 \rightarrow 2$ (see Figure 2). Also, in view of the lack of fundamental understanding of the point measurements, imaged thermometry was not attempted.

There are other possible ways to measure temperature in flames. Cattolica[20] has used a two-line method, in which the same upper state level is excited from two different lower rotational or vibrational levels. This avoids any problems due to collisional transfer and quenching, but does so at the expense of accuracy and dynamic range in the temperatures so obtained. If one understood the relative energy transfer and quenching rates as a function of N', these restrictions could be relaxed and different N' levels could be pumped. Much of the pertinent information on upper state OH transfer is contained in Refs. 5-7 and 15-19, but the present results on Q/V indicate a greater understanding is needed in order to use such an approach. Further research along such lines would be valuable, because a two-line method pumping different N' could be implemented with our recently demonstrated two-frame imaging method,[21] to provide an instantaneous map of the temperature field correlated with OH concentration.

IV PUBLICATIONS

The following journal articles and conference presentations have been supported by this contract.

A. Journal Articles

1. D. R. Crosley, "Laser-Induced Fluorescence in Spectroscopy, Dynamics, and Diagnostics," J. Chem. Educ., 59, 446 (1982).
2. M. J. Dyer and D. R. Crosley, "Two-Dimensional Imaging of OH Laser-Induced Fluorescence in a Flame," Optic Letters 7, 382 (1982).
3. D. R. Crosley and G. P. Smith, "Laser-Induced Fluorescence Spectroscopy for Combustion Diagnostics," Opt. Engr., 22, 545 (1983).
4. D. R. Crosley and M. J. Dyer, "Two-Dimensional Imaging of Laser-Induced Fluorescence in OH in a Flame," Proceedings of the International Conference on Lasers '82, 1983, p. 752.

B. Conference Presentations

1. D. R. Crosley, "Laser-Induced Fluorescence in Combustion Chemical Kinetics," Amer. Chem. Soc. Meeting, Las Vegas, Nevada, March 1982.
2. M. J. Dyer and D. R. Crosley, "Planar Imaging of OH Laser-Induced Fluorescence in an Atmospheric Pressure Flame," Paper 82-66, Western States Meeting of the Combustion Institute, Livermore, California, October 1982.
3. D. R. Crosley, "Laser-Induced Fluorescence Spectroscopy in Combustion Reseach," Bull. Amer. Phys. Soc. 27, 862 (1982).
4. D. R. Crosley and M. J. Dyer, "Two-Dimensional Imaging of Laser-Induced Fluorescence in OH in a Flame," Lasers '82, New Orleans, Louisiana, December 1982.
5. D. R. Crosley, "Laser-Induced Fluorescence for Combustion Chemistry," Bull. Amer. Phys. Soc. 28, 1341 (1983).

6. D. R. Crosley, "Laser Flame Diagnostics," Pittsburgh Conference on Analytical Chemistry and Applied Spectroscopy, Atlantic City, New Jersey, March 1984.

REFERENCES

1. D. R. Crosley, Ed., Laser Probes for Combustion Chemistry, Amer. Chem. Soc. Symposium Series, Vol. 134, 1980; D. R. Crosley and G. P. Smith, Opt. Engr. 22, 545 (1983).
2. M. J. Dyer and D. R. Crosley, Opt. Lett. 7, 382 (1982).
3. D. R. Crosley and M. J. Dyer, Proceedings of the International Conference on Lasers '82, 1983, p. 752.
4. D. R. Crosley and G. P. Smith, Appl. Opt. 19, 517 (1980).
5. G. P. Smith and D. R. Crosley, Appl. Opt. 22, 1428 (1983).
6. D. R. Crosley and G. P. Smith, Comb. Flame 44, 27 (1982).
7. R. K. Lengel and D. R. Crosley, Chem. Phys. Lett. 32, 261 (1975); J. Chem. Phys. 68, 5309 (1978).
8. We thank Richard R. Copeland for setting up the hardware and writing the programs enabling this mode of data acquisition.
9. We thank Philip L. Varghese for performing these calculations.
10. G. H. Dieke and H. M. Crosswhite, JQSRT 2, 97 (1962).
11. I. L. Chidsey and D. R. Crosley, JQSRT 23, 187 (1980).
12. D. R. Crosley and R. K. Lengel, JQSRT 15, 579 (1975).
13. We thank Philip L. Varghese for advice and instruction in the use of thermocouples and in performing the radiative corrections.
14. P. M. Doherty and D. R. Crosley, Appl. Opt. 23, 713 (1984).
15. I. S. McDermid and J. B. Laudenslager, J. Chem. Phys. 76, 1824 (1982).
16. R. A. Copeland and D. R. Crosley, Chem. Phys. Lett., in press, 1984.
17. R. A. Copeland, M. J. Dyer, and D. R. Crosley, to be published.
18. P. W. Fairchild, G. P. Smith, and D. R. Crosley, J. Chem. Phys. 79, 1795 (1983).
19. K. R. German, J. Chem. Phys. 64, 4065 (1976).
20. R. J. Cattolica, Appl. Opt. 20, 1156 (1981).
21. M. J. Dyer and D. R. Crosley, Opt. Lett., in press, 1984.

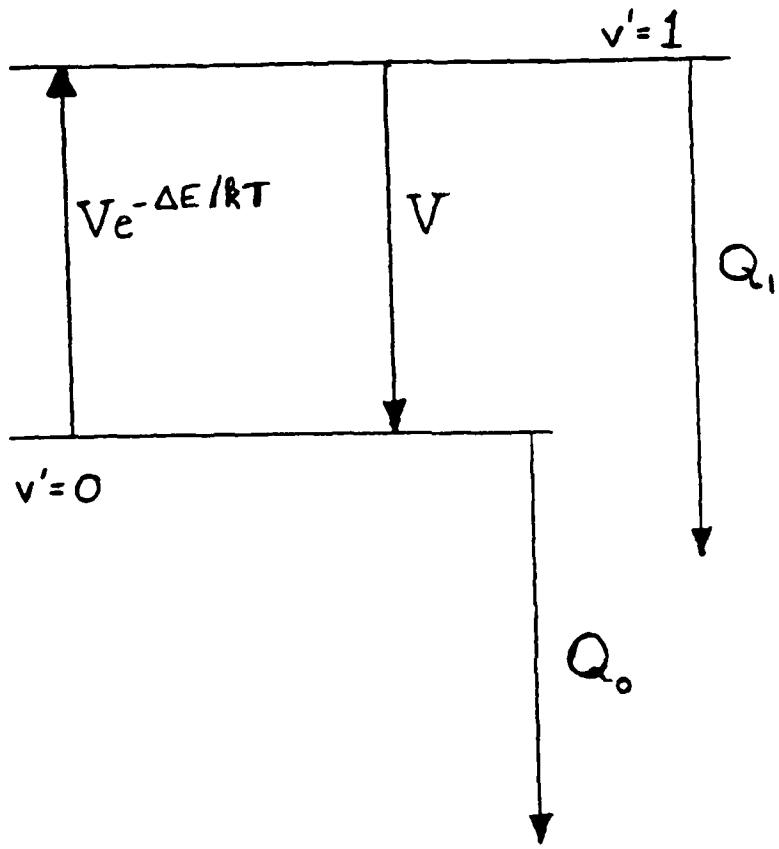

Figure 1. Schematic energy level diagram defining the energy transfer rates used in describing the energy transfer thermometry method.

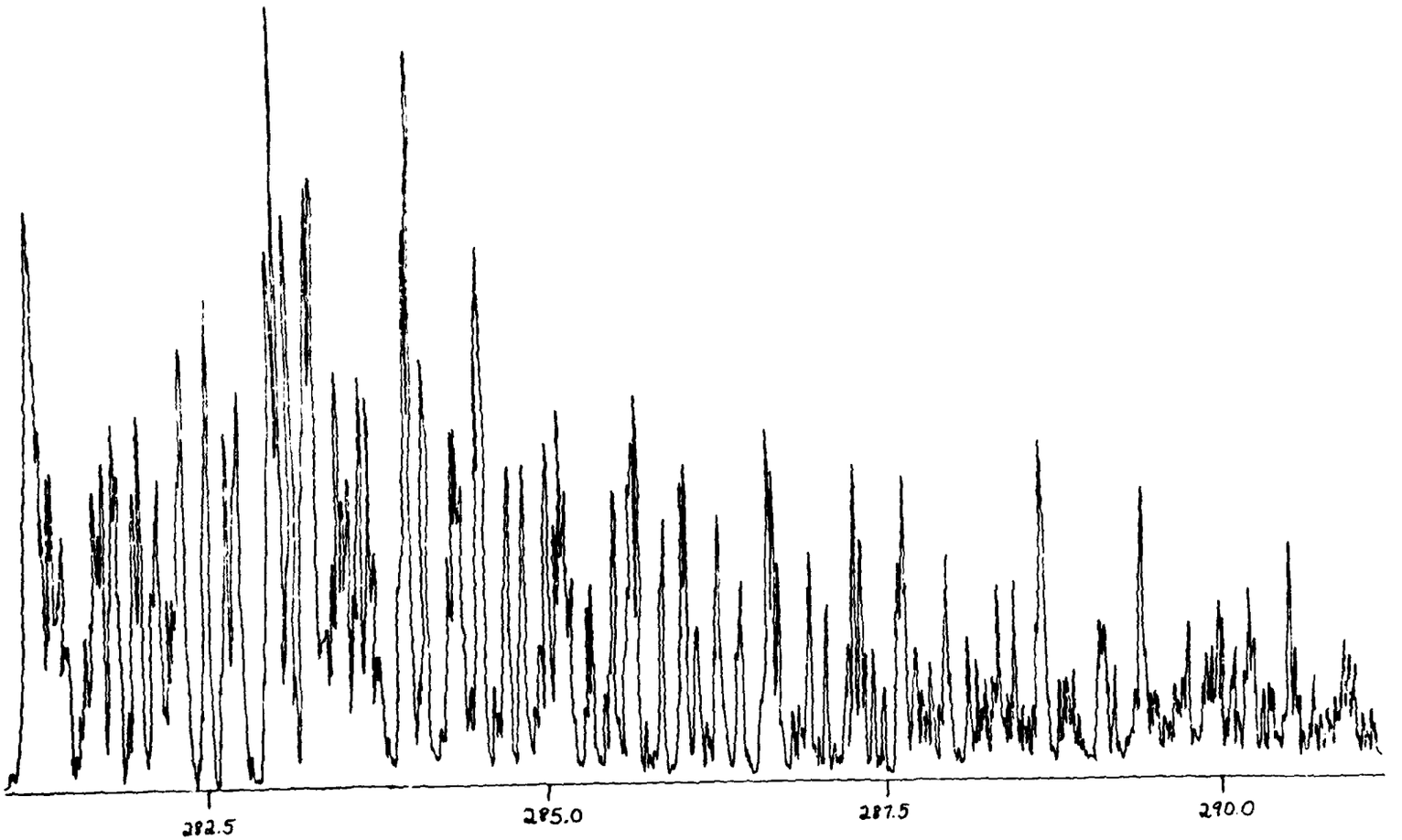

Figure 2. Rotationally resolved fluorescence scan of the (1,0) band, following uptransfer from v'=0 which is pumped. Resolution is 0.2 Å. The individual rotational lines can be identified using the tables of Dieke and Crosswhite, Ref. 10. 50 features involving levels through N'=15 were used in the analysis. The higher congestion of smaller features to the red of 287.5 nm is from the (2,1) band, also populated by upward collisional transfer.

Figure 3. Boltzmann plots of relative rotational populations in the v'=1 state following upward transfer. Triangles are F_1 levels and circles are F_2 levels. Top, $F_1(5)$ pumped in v'=0, 0.2 Å resolution, T=2020K. Middle, $F_1(5)$ pumped, 0.8 Å, T=1900K. Bottom, $F_2(11)$ pumped, 0.8 Å, T=2130K.

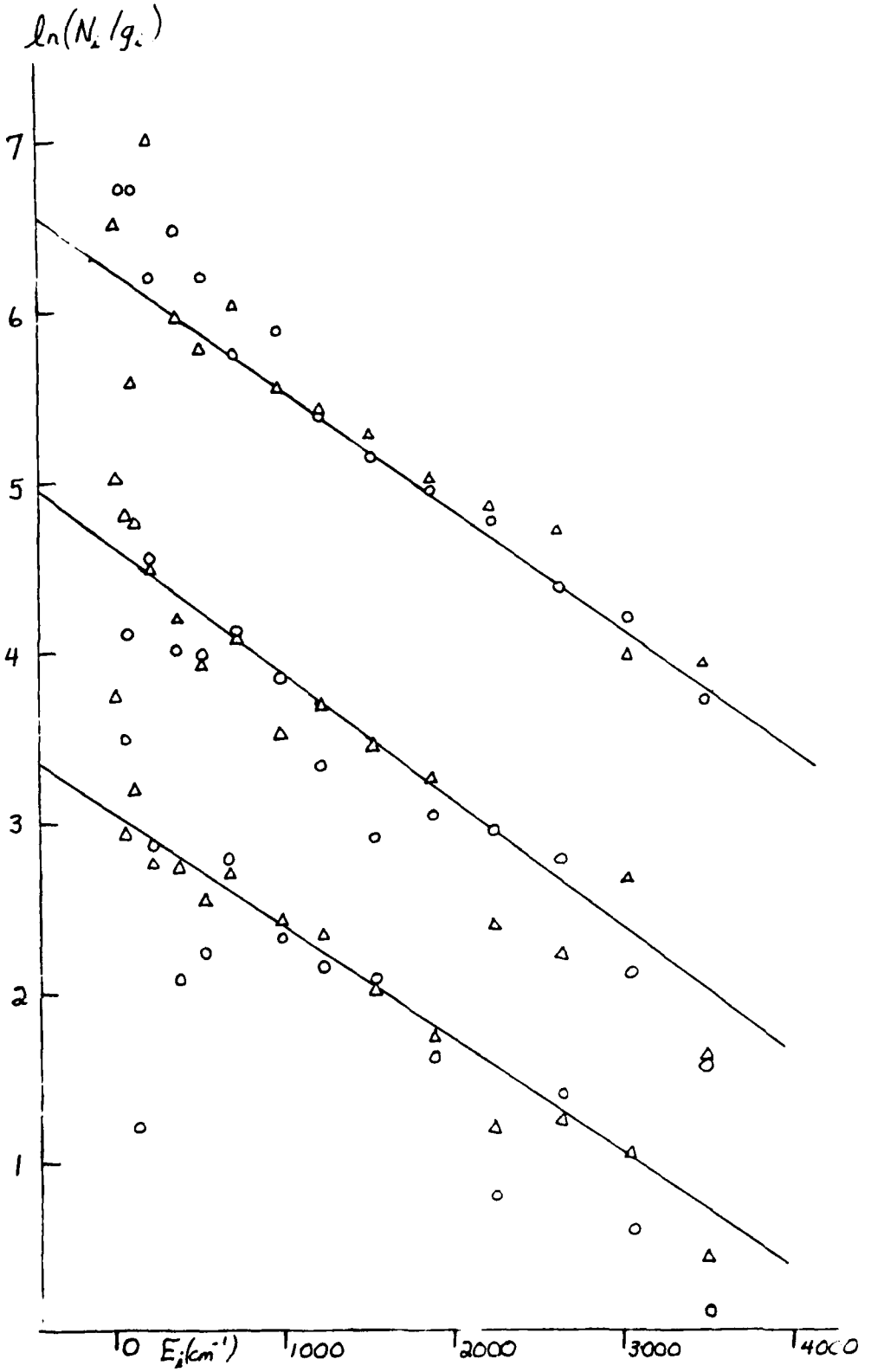

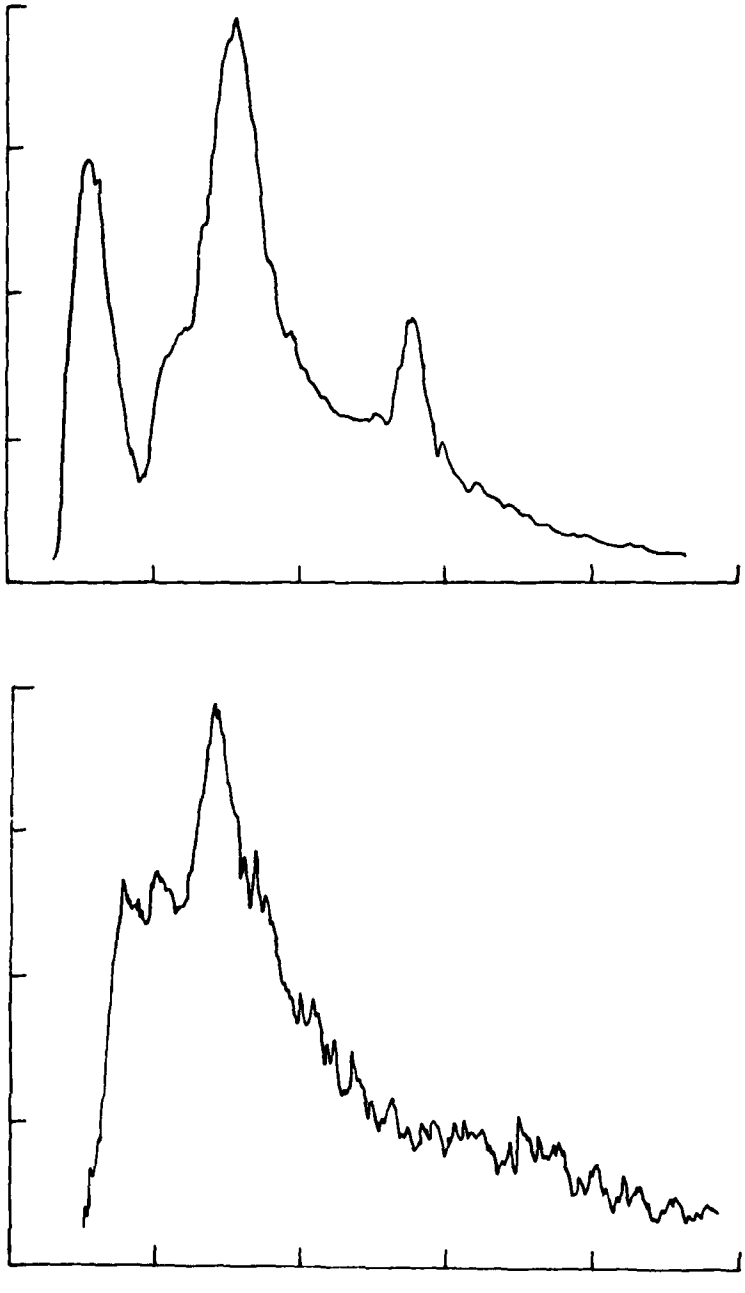

Figure 4. Exemplary thermometry runs as stored on the computer. Plotted is intensity vs wavelength of the spectrometer, which is operated in low resolution. Top, (0,0) band, initially pumped; bottom, (1,0) band populated by upward transfer. The intensity scale for the lower run is a factor of 37.5 more sensitive than in the upper scan. Integrated intensities are used for the data analysis.

Figure 5. Exemplary Boltzmann plots of rotational populations in the ground state of OH, obtained by excitation scans and used to determine the rotational temperature T_R. Circles and triangles denote two separate series of runs; lines represent least-squares fits. The corresponding temperatures are: circles, 1998K, triangles, 2025K.

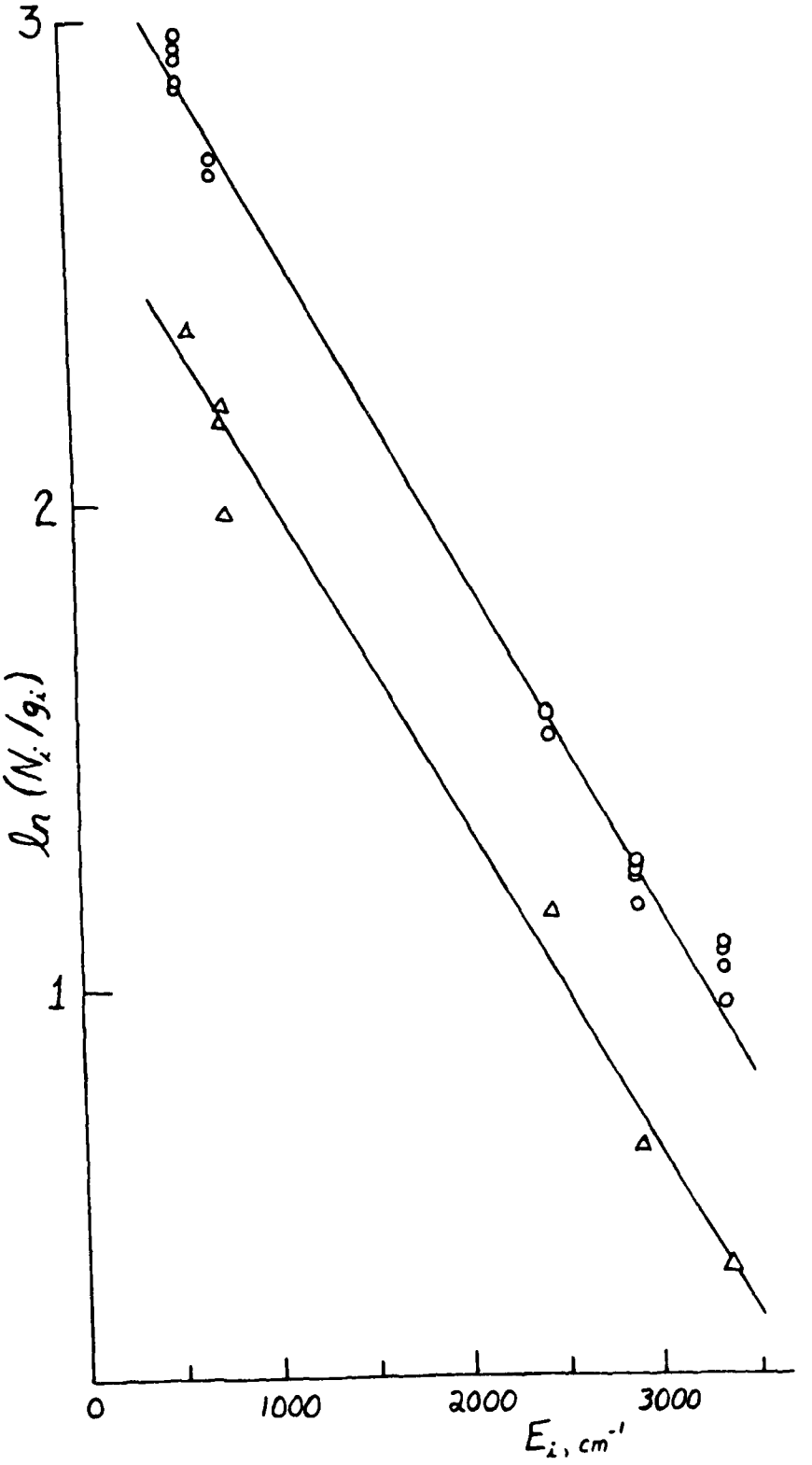

Figure 6. Thermocouple measurements as a function of burner height for flame M. These are the directly measured values before radiative corrections. The flame zone reaches its T_{max} at x=6.75 cm; smaller values of x are positions higher in the burnt gases. The single point at x=4.5 illustrates T calculated there applying the fitted radiative correction method described in the text. The error bars represent its uncertainty from the scatter in corrected T from the different thermocouples. At T > 2000K the thermocouples do not survive, precluding measurements.

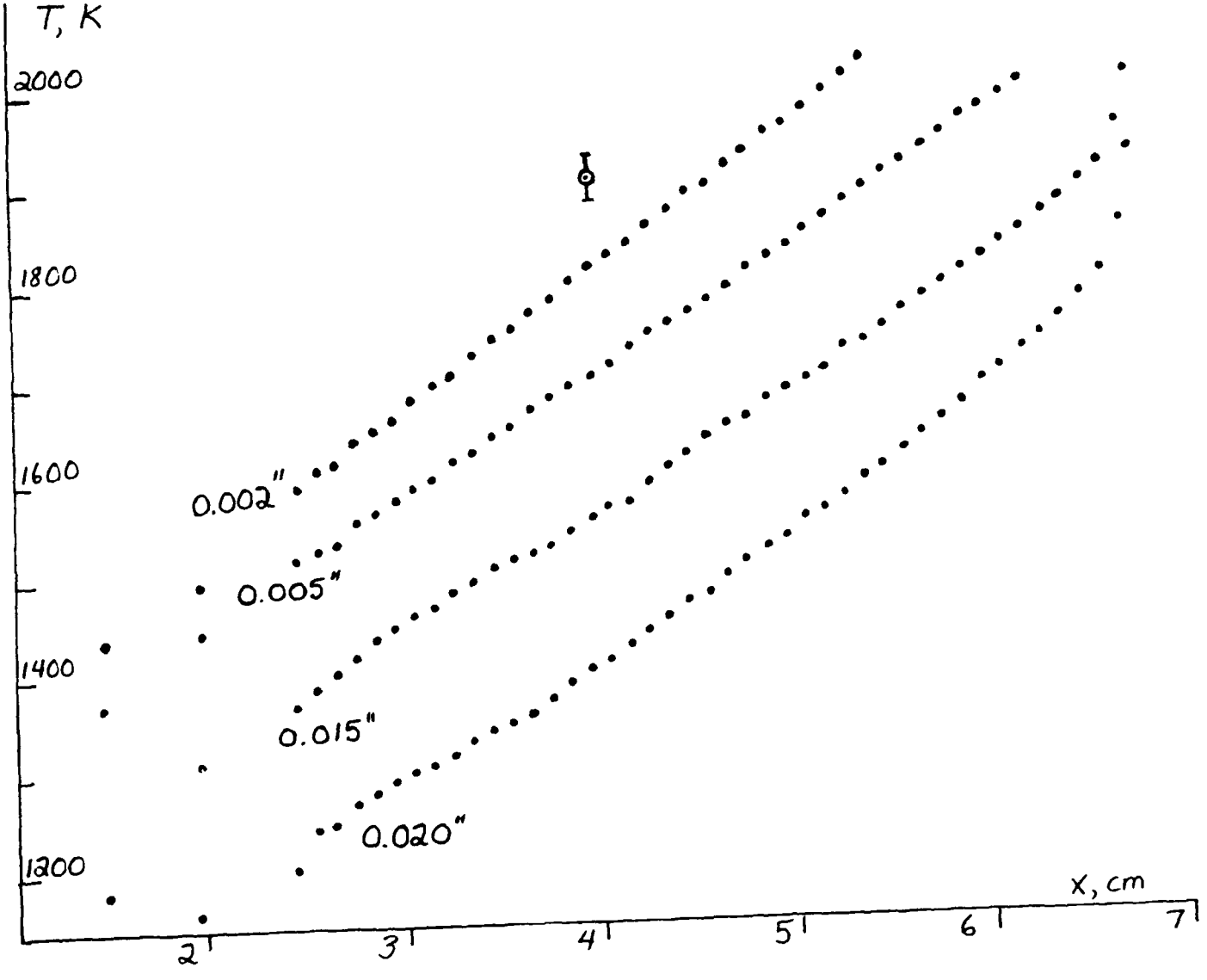

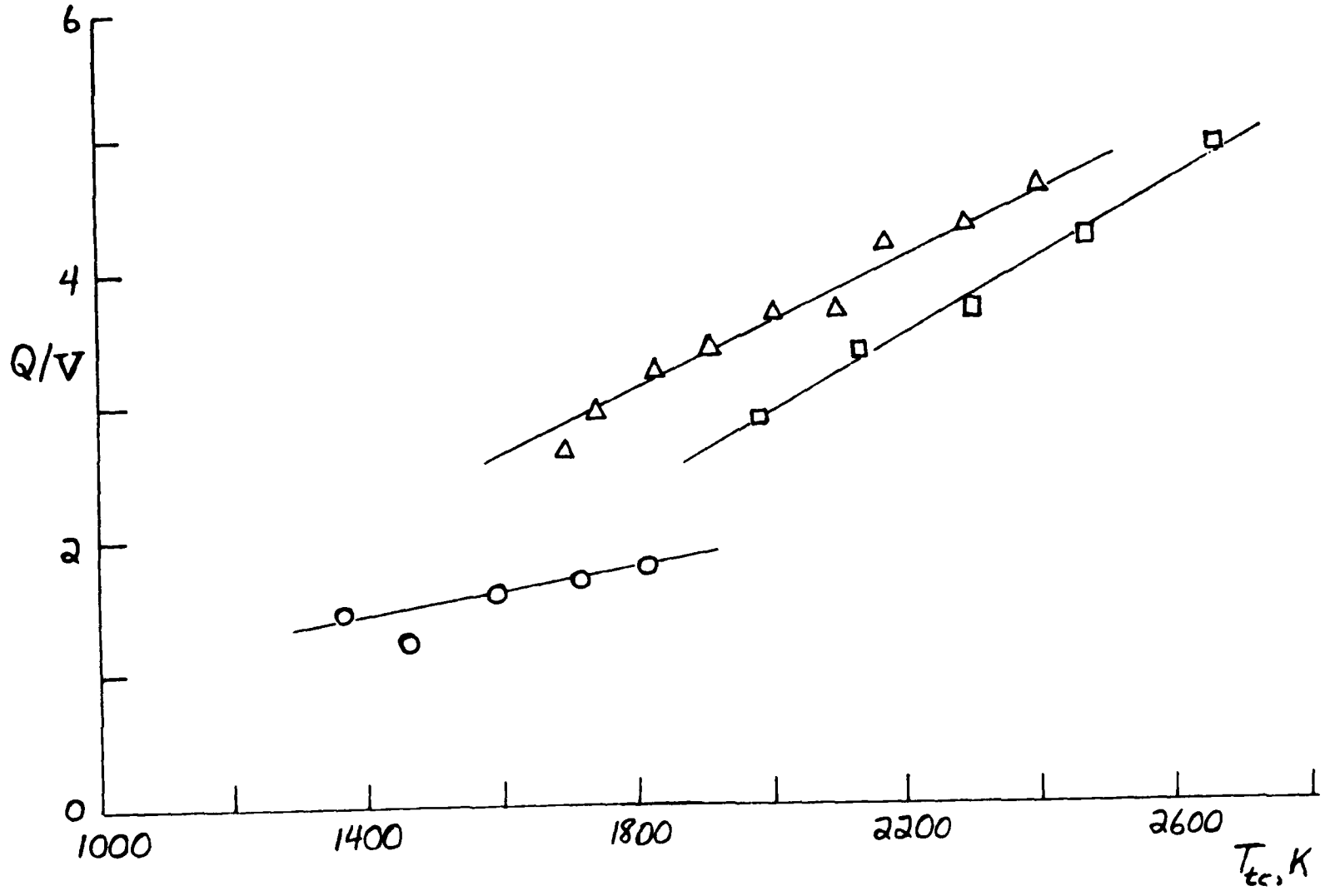

Figure 7. Measured Q/V results as a function of T_{tc} for the three flames: circles, flame L; triangles, flame M; squares, flame H. The lines serve merely to connect the points for each flame for ease of seeing the trends.

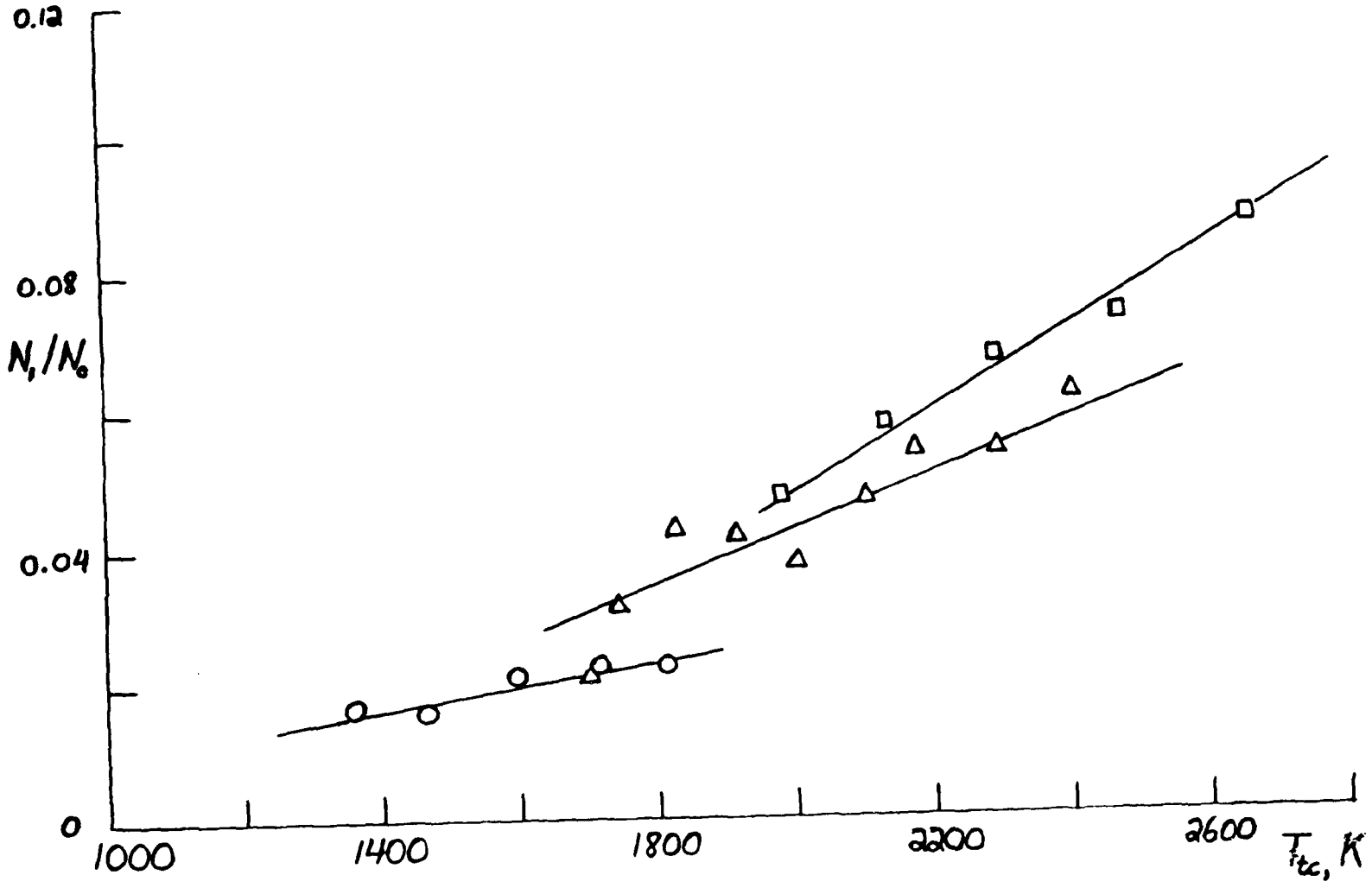

Figure 8. Measured upward transfer ratios N_1/N_o as a function of T_{tc}; circles, L; triangles, M; squares, H. As in Figure 7, the lines serve to illustrate the trends.

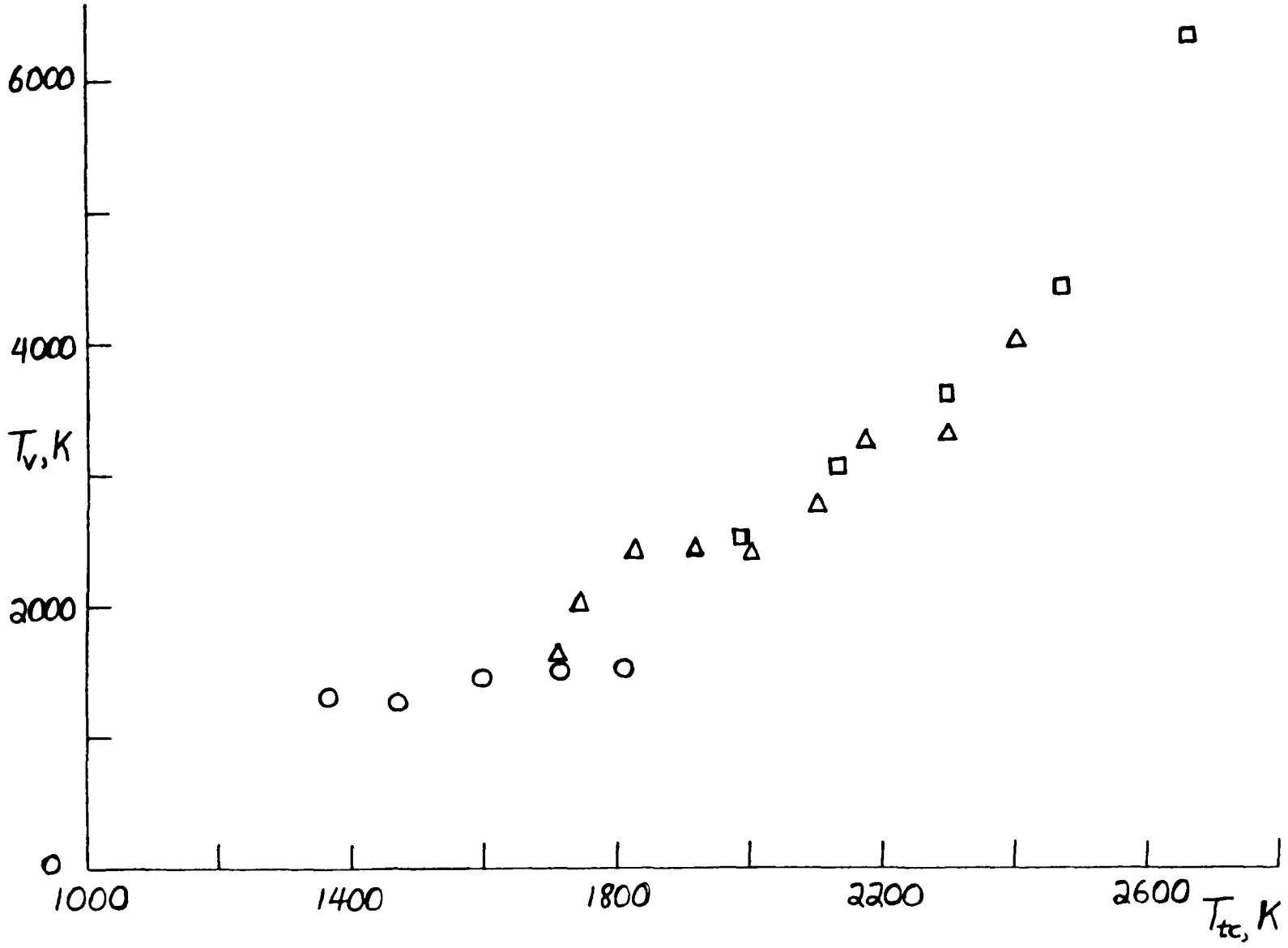

Figure 9. Thermometry results T_V as a function of T_{tc}; circles, L; triangles, M; squares, H. The T_V is obtained using Eq. 3 and the measured values of Q/V and N_1/N_o plotted in Figures 7 and 8, respectively, as described in the text.

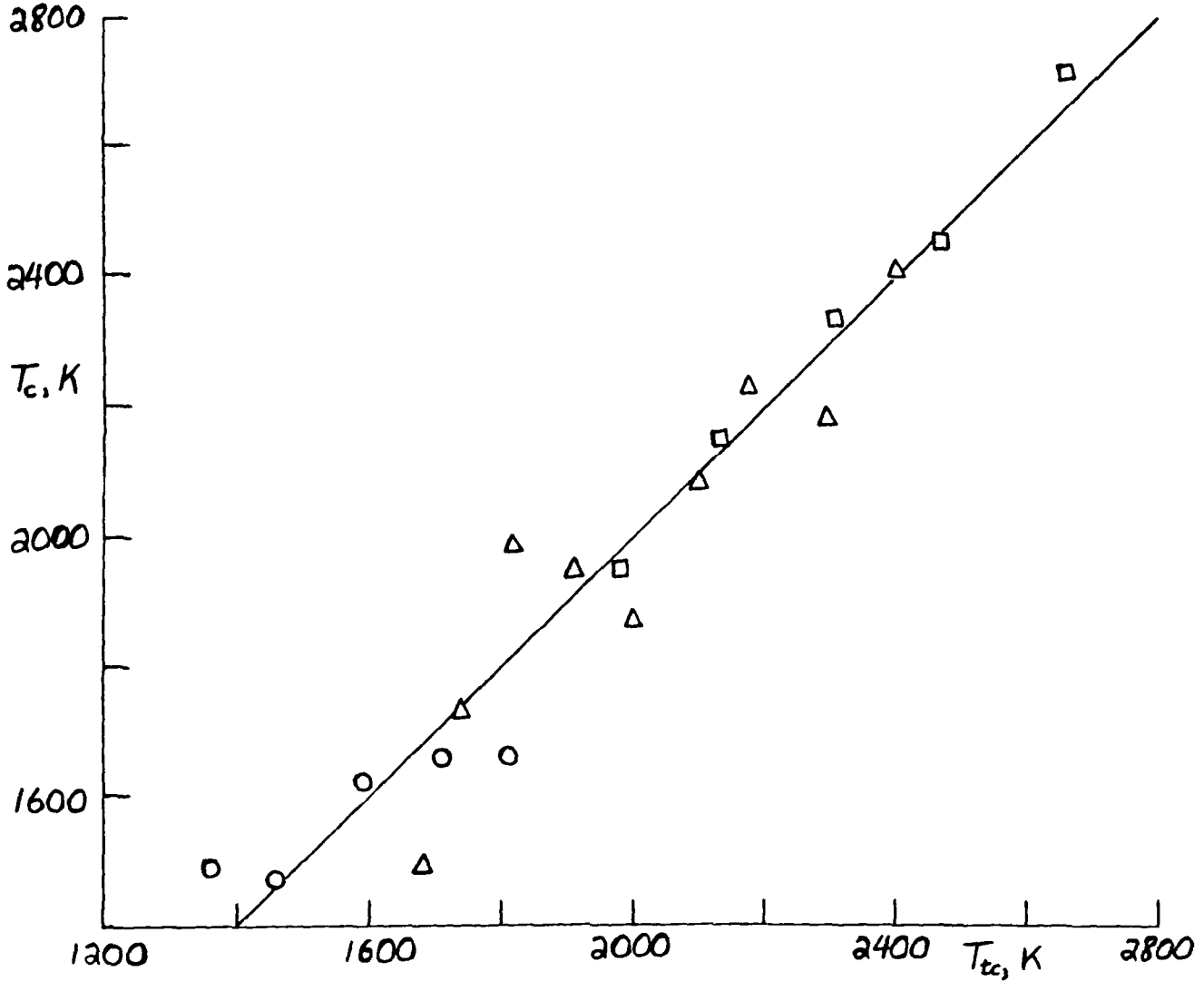

Figure 10. "Calibrated" temperature T_C using average values of Q/V for each flame, as described in the text, as a function of T_{tc}. Circles, L; triangles, M; squares, H. The straight line is a plot of the equation $T_C=T_{tc}$, which corresponds to an exact measurement.

END

FILMED

2-85

DTIC